articles

molecular pharmaceutics

Development of a Genetically Engineered Biomimetic Vector for Targeted Gene Transfer to Breast Cancer Cells

Sriramchandra S. Mangipudi, Brenda F. Canine, Yuhua Wang, and Arash Hatefi*

Department of Pharmaceutical Sciences, Center for Integrated Biotechnology, Washington State University, Pullman, Washington 99164

Received December 2, 2008; Revised Manuscript Received April 13, 2009; Accepted May 6, 2009

Abstract: A biomimetic vector was genetically engineered to contain at precise locations (a) an adenovirus μ peptide to condense pDNA into nanosize particles, (b) a synthetic cyclic peptide to target breast cancer cells and enhance internalization of nanoparticles, (c) a pH-responsive synthetic fusogenic peptide to disrupt endosome membranes and facilitate escape of the nanoparticles into the cytosol, and (d) a nuclear localization signal from human immunodeficiency virus for microtubule mediated transfer of genetic material to the nucleus. The vector was characterized using physicochemical and biological assays to demonstrate the functionality of each motif in the vector backbone. The results demonstrated that the vector is able to condense plasmid DNA into nanosize particles (<100 nm), protect pDNA from serum endonucleases, target ZR-75-1 breast cancer cells and internalize, efficiently disrupt endosome membranes, exploit microtubules to reach nucleus and mediate gene expression. The therapeutic potential of the vector was evaluated by complexing with plasmid DNA encoding TRAIL (pTRAIL) and transfecting ZR-75-1 cells. The results demonstrated that up to 62% of the ZR-75-1 breast cancer cells can be killed after administration of pTRAIL in complex with the vector.

Keywords: Biomimetic vector; nonviral vector; cancer gene therapy

1. Introduction

Gene therapy is perceived as a ground-breaking technology with the promise to cure almost any disease, provided that we understand its genetic and molecular basis. However, enthusiasm has rapidly abated as multiple clinical trials failed to show efficacy. The limiting factor seems to be the lack of a suitable delivery system to carry the therapeutic genes safely and efficiently to the target tissue.[1] Gene-transfer technology is still in a nascent stage owing to several inherent limitations in the existing delivery methods. Viral vectors are the vehicles of choice for cancer gene therapy particularly due to their ability to overcome the intracellular barriers and the enormous possibility for recombinant engineering. However, nonspecific binding to all cells that overexpress coxsackievirus and adenovirus receptor (CAR), potential immunogenicity, high costs of production, and the fact that the majority of cancer cells do not express CAR has limited their use for cancer gene therapy.[2,3] To overcome these problems, nonviral vectors such as cationic lipids and polymers have been developed. While lipoplexes provide relatively high transfection efficiency, their large scale production, reproducibility and cytotoxicity remain major concerns.[4] On the other hand, cationic polyplexes are robust and relatively biocompatible but they are marred by poor gene-transfer efficiency.[5] What has been long sought after is a

* Correspondence should be addressed to Arash Hatefi (e-mail: ahatefi@wsu.edu), Department of Pharmaceutical Sciences Center for Integrated Biotechnology, Washington State University, P.O. Box 646534, Pullman, WA 99164. Phone: 509-335-6253. Fax: 509-335-5902.

(1) Louise, C. Nonviral vectors. *Methods Mol. Biol.* **2006**, *333*, 201–26.

(2) Thomas, C. E.; Ehrhardt, A.; Kay, M. A. Progress and problems with the use of viral vectors for gene therapy. *Nat. Rev. Genet.* **2003**, *4*, 346–58.

(3) Shen, Y.; Nemunaitis, J. Herpes simplex virus 1 (HSV-1) for cancer treatment. *Cancer Gene Ther.* **2006**, *13*, 975–92.

(4) Lv, H.; Zhang, S.; Wang, B.; Cui, S.; Yan, J. Toxicity of cationic lipids and cationic polymers in gene delivery. *J. Controlled Release* **2006**, *114*, 100–9.

10.1021/mp800251x CCC: $40.75
Published on Web 05/06/2009

technology which combines biocompatibility, efficiency, and engineerability in a single effective gene-transfer technology platform. An alternative recombinant biomimetic nonviral approach is on the horizon, but it is not without its own inherent challenges. Significant amounts of preliminary groundwork have been done addressing the feasibility concerns of this approach.[6−10]

Herein, we report a fusion vector which is composed of multiple functional motifs for targeted gene transfer. The first generation of this type of gene delivery system, namely, designer biomimetic vector (DBV), is based on a one-domain−one-function architecture concept. While viruses delegate different functions to multiple peptide subunits, the nonviral DBV reported here embeds several functional domains onto a single module (biomacromolecule). Using this approach, the vector is programmed via its amino acid sequence to perform a selection of self-guided functions. These include (a) efficient condensation of the plasmid DNA (pDNA) into deliverable nanoparticles by a DNA condensing motif (DCM) obtained from adenovirus μ peptide,[11] (b) cell-specific delivery of the nanoparticles using a combinatorially screened cyclic targeting peptide (TP),[12] (c) endosomal disruption by an engineered pH-responsive endosome disrupting motif (EDM) mimicking influenza virus fusogenic peptide,[13] and finally (d) microtubule assisted transport of the genetic material toward the nucleus for efficient gene expression by a nuclear localization signal (NLS) obtained from human immunodeficiency virus type 1 (HIV-1).[14]

We hypothesize that the proposed DBV is able to condense pDNA into nanosize particles, protect pDNA from degradation by serum endonucleases, target model cancer cells and internalize via receptor-mediated endocytosis, disrupt endosome membranes to escape into the cell cytoplasm, exploit microtubules to facilitate translocation of the genetic material across the cytoplasm toward the nucleus, and ultimately mediate gene transfer. In this study, the word "transfection efficiency" encompasses both percent transfected cells and total green fluorescent protein expression.

2. Materials and Methods

2.1. Cloning, Expression, and Purification of DBV. The gene encoding DBV with an N-terminal histag was designed in our lab, custom synthesized by Integrated DNA Technologies, Inc., and provided in pZErO plasmid. The resident DBV gene flanked on either side by *Nde*I and *Xho*I restriction sites was cloned into a pET21b expression vector under the control of a T7 promoter. The resultant expression construct pET21b:DBV was tested for its fidelity to the original design by DNA sequencing.

The pET21b:DBV expression vector was transformed into *Escherichia coli* BL21(DE3) pLysS. Starter cultures, 5 mL, were then grown in LB media at 37 °C overnight with 50 μg/mL carbenicillin. Circlegrow media (MB Biomedicals, Solon, OH), 500 mL, was inoculated with the starter culture and allowed to grow at 30 °C until the absorbance reached 3.0 at 600 nm. The culture was inducted with 0.4 mM IPTG for 2 h. The culture broth was centrifuged at 6000 rpm for 7 min at 4 °C, and the pellet was frozen until further use.

The pellet was suspended in lysis buffer containing 100 mM NaH_2PO_4, 10 mM Tris-HCl (pH 8.0), and 6 M guanidinium hydrochloride and the lysate was centrifuged at 18000 rpm for 60 min. For purifying the dimer no reducing agent was used, whereas for the purification of the monomer 12 mM 2-mercaptoethanol was used in all buffers. The soluble fraction was adjusted to 12 mM imidazole, and 0.5 mL of Ni-NTA resin equilibrated in the same buffer was added. The expressed DBV was allowed to bind in a batch mode for 60 min at room temperature. The tubes were centrifuged at 1000*g* for 5 min, and the supernatant was discarded. The resin was loaded in a 0.8 × 4 cm BioRad PolyPrep chromatography column, washed with 25 mL of lysis buffer supplemented with 15 mM imidazole, and eluted with 250 mM imidazole. The DBV was stored in 50% glycerol at −20 °C. The purity and expression of the DBV were determined by SDS−PAGE and Western blot analysis (monoclonal anti-6XHis), respectively. The monomer and dimer were loaded onto the SDS−PAGE gel using a loading buffer without reducing agent. Using the same genetic engineering protocol mentioned above, the DBV without NLS was also expressed and purified.

2.2. Preparation of DBV Stock Solution. Before use, DBV was precipitated out of the storage buffer by adding saturated ammonium sulfate solution (4.2 M) in small

(5) Pack, D. W.; Hoffman, A. S.; Pun, S.; Stayton, P. S. Design and development of polymers for gene delivery. *Nat. Rev. Drug Discovery* **2005**, *4*, 581–93.
(6) Fominaya, J.; Uherek, C.; Wels, W. A chimeric fusion protein containing transforming growth factor-alpha mediates gene transfer via binding to the EGF receptor. *Gene Ther.* **1998**, *5*, 521–30.
(7) Paul, R. W.; Weisser, K. E.; Loomis, A.; Sloane, D. L.; LaFoe, D.; Atkinson, E. M.; Overell, R. W. Gene transfer using a novel fusion protein, GAL4/invasin. *Hum. Gene Ther.* **1997**, *8*, 1253–62.
(8) Uherek, C.; Fominaya, J.; Wels, W. A modular DNA carrier protein based on the structure of diphtheria toxin mediates target cell-specific gene delivery. *J. Biol. Chem.* **1998**, *273*, 8835–41.
(9) Canine, B. F.; Wang, Y.; Hatefi, A. Evaluation of the effect of vector architecture on DNA condensation and gene transfer efficiency. *J. Controlled Release* **2008**, *129*, 117–123.
(10) Hatefi, A.; Megeed, Z.; Ghandehari, H. Recombinant polymer-protein fusion: a promising approach towards efficient and targeted gene delivery. *J. Gene Med.* **2006**, *8*, 468–76.
(11) Keller, M.; Tagawa, T.; Preuss, M.; Miller, A. D. Biophysical characterization of the DNA binding and condensing properties of adenoviral core peptide mu. *Biochemistry* **2002**, *41*, 652–9.
(12) Dane, K. Y.; Chan, L. A.; Rice, J. J.; Daugherty, P. S. Isolation of cell specific peptide ligands using fluorescent bacterial display libraries. *J. Immunol. Methods* **2006**, *309*, 120–9.
(13) Midoux, P.; Kichler, A.; Boutin, V.; Maurizot, J. C.; Monsigny, M. Membrane permeabilization and efficient gene transfer by a peptide containing several histidines. *Bioconjugate Chem.* **1998**, *9*, 260–7.
(14) Cochrane, A. W.; Perkins, A.; Rosen, C. A. Identification of sequences important in the nucleolar localization of human immunodeficiency virus Rev: relevance of nucleolar localization to function. *J. Virol.* **1990**, *64*, 881–5.

increments while incubating on ice. The salted out vector was collected in a microfuge tube by centrifugation at 5000*g* and removal of supernatant. Subsequently, DBV was redissolved in 10 mM bis-tris propane buffer (pH 7) to make ca. 2.0 mg/mL stock solution. This stock solution was used in ensuing studies.

2.3. Hemolysis Assay. Two milliliters of sheep red blood cells (Innovative Research, Novi, MI) was washed several times with phosphate buffered saline (PBS). Cell numbers were adjusted to 3.2×10^8 cells/mL in Dulbecco's PBS at pH 7.4 and 7.0 or 50 mM acetate buffer at pH 5.0, adjusted to physiological ionic strength with NaCl. The cell suspension in buffers was supplemented with 1, 10, 20, or 30 μg of the vector. The mixture was incubated at 37 °C for 1 h and centrifuged, and the absorbance of the supernatant was measured at 541 nm. Triton X-100 (1%) was used as the positive control, and phosphate and acetate buffers were used as negative controls. The percentage of hemolysis for the test groups (dimer) is reported as relative to fully lysed cells by Triton X-100 (defined as 100%). Data is reported as mean $\pm$ SD, $n = 3$. The statistical significance was tested using *t* tests ($p < 0.05$).

2.4. Particle Size Analysis. Vectors were complexed with plasmid DNA encoding green fluorescent protein (pEGFP Clontech, California) at various N:P ratios (the molar ratio of positively charged nitrogen atoms to negatively charged phosphates in pDNA). We did not consider conditionally positively charged histidine residues for N:P ratio calculations. Complexation was achieved by adding various amounts of vector solution in 10 mM bis-tris propane buffer (pH 7) to an equal volume of buffer containing 1 μg of pEGFP. For example, at an N:P ratio of 10, 20 μg of vector was complexed with 1 μg of pEGFP. The mean hydrodynamic particle size measurements for vector/pDNA complexes were performed using dynamic light scattering (DLS) by a Malvern Nano ZS90 instrument and DTS software (Malvern Instruments, U.K.). The data is reported as mean $\pm$ SEM, $n = 3$. Each mean is an average of 15 measurements, and *n* represents the number of independent batches prepared for size measurements.

2.5. Particle Stability in Serum. The stability of the nanoparticles in the presence of serum was examined using gel retardation assay. In one set of tubes, 1 μg of pEGFP was complexed with the vector (dimer), incubated at room temperature for 15 min, and the mobility of pDNA was visualized by ethidium bromide staining and agarose gel electrophoresis. In the second set, particles were formed by complexing 1 μg of pEGFP with the vector followed by addition of fetal bovine serum (Invitrogen, California) at the final concentration of 10% (v/v). The complexes were incubated for 90 min at 37 °C in the presence of serum and then electrophoresed on a 1% agarose gel. The pDNA mobility was visualized by ethidium bromide staining.

To evaluate the ability of the vector (dimer) in protecting pDNA from endonucleases, complexes were formed at an optimal N:P 10 in a microfuge tube and incubated with serum for 90 min. Subsequently, sodium dodecyl sulfate was added (10%) to the tubes to release the pDNA from the vector. Samples were electrophoresed on agarose gel and visualized by ethidium bromide staining.

2.6. Transmission Electron Microscopy. The vector was complexed with pEGFP, and nanoparticles were prepared at N:P 10 on Formvar coated grids and stained with uranyl acetate for 5 min. The nanoparticles were imaged using JEOL 1200 EX II (120 kV).

2.7. Cell Culture and Transfection. ZR-75-1 (ATCC, Manassas, VA) breast cancer cells were seeded in 96 well tissue culture plates in RPMI 1640 supplemented with 10% serum at a density of 5×10^4 cells per well. MDA-MB-231 breast cancer cells and MCF-10A (ATCC, Manassas, VA) normal human mammary cells were seeded in 96 well tissue culture plates in MEBM complete media at 3×10^3 cells per well. Cells were approximately 80% confluent at the time of transfection. ZR-75-1 cells were transfected in the presence of RPMI-1640 supplemented with 10% fetal bovine serum and in serum free media (RPMI-1640 supplemented with insulin−transferrin−selenium, dexamethasone, and fibronectin human plasma). A 100 μL aliquot of vector/pEGFP complex at various N:P ratios (1 to 16) containing 1 μg of pEGFP was added to each well, and the plates were incubated for 2 h in CO_2 incubator at 37 °C. After 2 h, the medium was removed and replaced with RPMI 1640 supplemented with 10% (v/v) serum. When used, chloroquine (100 μM), bafilomycin A1 (10nM), or nocodazole (10 μM) were added. The expression of GFP was visualized after 48 h by an epifluorescent microscope (Zeiss Axio Observer Z1). The percent transfected cells and total green fluorescent protein expression were determined by flow cytometry (FacsCalibur, Becton Dickinson, San Jose, CA). Vector without NLS in complex with pEGFP was used as a control to examine the role of NLS. Lipofectamine 2000 (Invitrogen, Carlsbad, CA) was used as a positive control to validate the transfection process. Lipofectamine was complexed with pEGFP in Opti-MEM (Invitrogen) as per manufacturer's protocol and used to transfect cells. The data are presented as mean $\pm$ SD, $n = 3$. The statistical significance was evaluated using a *t* test ($p < 0.05$).

2.8. Inhibition Assay. Cells were seeded at a density of 5×10^4 cells per well in a 96 well plate. Aliquots of targeting peptide in serum free media were added at concentrations of 0, 0.07, 0.7, 1.4, 2.8, and 5.5 nM to the wells. The plates were placed at 37 °C in CO_2 incubator for 1 h with intermittent mixing at intervals of 15 min. Aliquots of dimer (100 μL) in complex with 1 μg of pEGFP at N:P 10 were added to each of the wells. The control well with 0 μg/mL concentration received PBS. The measured percent transfected cells for the test groups (pretreated with targeting peptide) are expressed as percent of the control (untreated) defined as 100%. The targeting peptide was synthesized using solid phase peptide synthesis by Anaspec Inc. (San Jose, CA). The data are shown as mean $\pm$ SD, $n = 3$. The statistical significance was examined using a *t* test ($p < 0.05$).

2.9. Cancer Cell Killing Efficiency. This assay was performed in serum free media on ZR-75 cells for the vector

(dimer), vector/pEGFP complexes (N:P 10), and vector/pTRAIL-GFP (N:P 10). ZR-75-1 cells were seeded at a density of 5×10^4 cells per well in 96 well plates. Cells were treated with serial dilutions of vector alone, vector in complex with pEGFP or vector/pTRAIL-GFP complexes for two hours. Plasmid DNA encoding tumor necrosis factor related apoptosis inducing ligand fused to GFP (pTRAIL-GFP) was kindly provided by Dr. Forrest at the University of Kansas. Subsequently, the media was removed and replaced with fresh RPMI supplemented with 10% serum followed by overnight incubation at 37 °C in a humidified CO_2 atmosphere. The control well with 0 μg/mL concentration received PBS. After 48 h, WST-1 reagent (Roche Applied Science, Indianapolis, IN) was added and incubated for 4 h, and absorbance was measured at 440 nm. The measured absorbance for test groups is expressed as percent of the control where the control is defined as 100% viable. Lipofectamine in complex with pTRAIL-GFP was used as positive control. The expression of TRAIL-GFP was confirmed using an epifluorescent microscope. The data are reported as mean $\pm$ SD, $n = 3$. The statistical significance was determined using a t test ($p < 0.05$).

3. Results

3.1. Cloning, Expression, and Purification of DBV. The gene encoding the vector, namely, DBV, was cloned into a pET21b expression vector to make pET21b:DBV, and the sequence of the gene was verified by DNA sequencing. The results showed no signs of deletion or mutation during the cloning process. The expression system was transformed into *E. coli* BL21 (DE3) plysS, and DBV was expressed and purified at a 2 mg/L yield. Due to the cyclic nature of the targeting peptide, the DBV was engineered to stably exist as a monomer or dimer. The general structure of the vector and sequence of each motif are shown in Figure 1.

The purity and expression of DBV in both monomer (molecular weight: 11.4 kDa) and dimer (molecular weight: 22.8 kDa) configurations with high purity were confirmed by SDS−PAGE and Western blot analysis, respectively (Figure 2a). We have previously established and reported the technology to produce highly cationic vectors in *E. coli* under similar conditions.[9,10]

3.2. Hemolysis Assay. The results of hemolysis assay demonstrated that the vector does not induce significant membrane lysis at pH 7.4 in the range tested (1−30 μg) (Figure 2b). At pH 7.0 and concentrations below 10 μg no significant hemolytic activity was observed in comparison to negative control. However, as the concentration increased, the hemolytic activity at pH 7.0 also increased. In comparison to negative control, the vector demonstrated significant hemolytic activity at pH 5.0 and at concentrations ≥ 10 μg.

3.3. Particle Shape and Size Analysis. The TEM images show that the vector/pEGFP complexes are compact spherical nanoparticles with 60−70 nm size (only dimer is shown; Figure 3a).

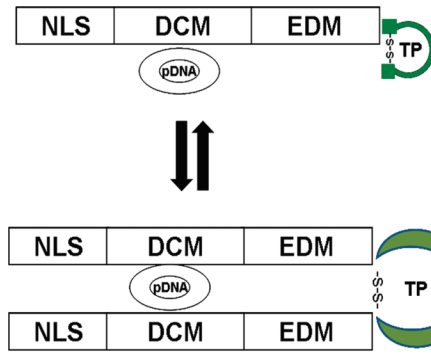

Figure 1. Schematic representation of the designer biomimetic vectors. The vector (monomer) is composed of a nuclear localization signal (NLS), a DNA condensing motif (DCM), an endosome disrupting motif (EDM), and a cyclic targeting peptide (TP). The dimer is created through the linkage of cysteine residues in targeting peptide via disulfide bonds. The amino acid sequence of each domain is also shown.

The results of particle size analysis showed that both dimer and monomer were able to efficiently condense pEGFP into nanoparticles with average sizes below 100 nm at N:P ratios between 4 and 10 (Figure 3b).

3.4. Determination of Optimum N:P Ratio for Transfection. ZR-75-1 cells were transfected in the absence of serum with the vector/pEGFP complexes formed with monomer and dimer at various N:P ratios. While GFP expression was observed for both monomer and dimer at all N:P ratios (data not shown), the highest level of transfection efficiency was observed at N:P 10 (Figure 4a). We did not observe any significant difference between the transfection efficiency of dimer versus monomer at this N:P ratio. Although the total green fluorescent expression with dimer seems slightly higher than Lipofectamine, the difference is not statistically significant ($p = 0.14$) (Figure 4a).

ZR-75-1 cells were also transfected in the presence of serum with DBV/pEGFP complexes at an N:P ratio of 10. The results showed no significant difference in percent transfected cells or total green fluorescent expression in the presence or absence of serum (data not shown).

3.5. Particle Stability in Serum. The vector (dimer) was complexed with pEGFP at N:P 10 and examined for its ability to protect pDNA from serum endonucleases. The results showed that these particles were stable in the absence and presence of 10% serum (Figure 4b, lanes 2 and 3) and effectively protected pDNA from degradation by the serum nucleases (Figure 4b, lane 4).

3.6. Evaluation of the Functionality of TP. An inhibition assay was performed to demonstrate internalization of the nanoparticles via the receptors that correspond to the targeting peptide. The results of this assay revealed that as the concentration of the targeting peptide (competitive inhibitor) increased, the levels of gene expression decreased

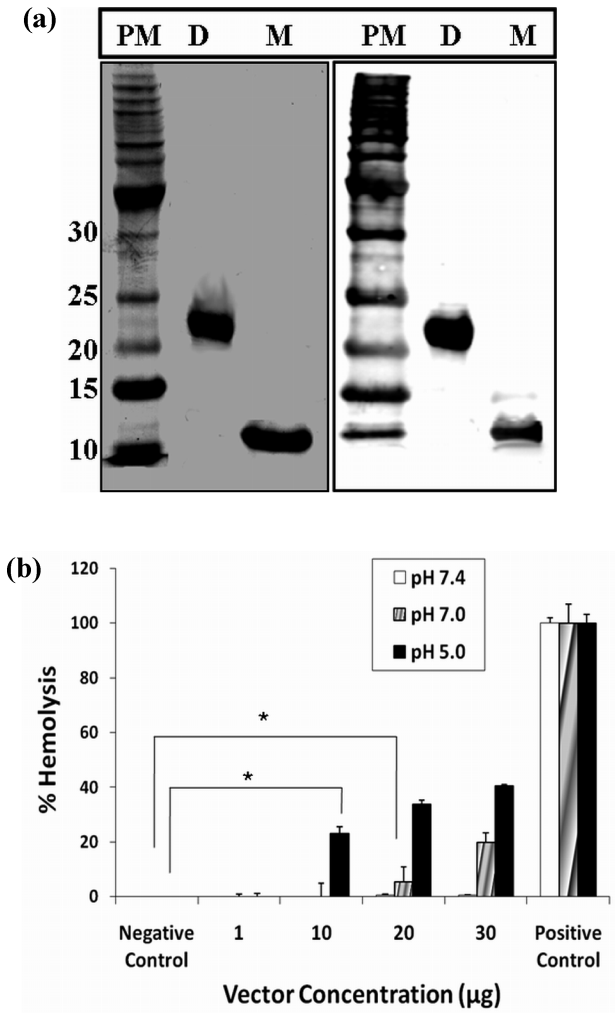

Figure 2. Expression and characterization of the DBV. (a) SDS−PAGE (left panel) and Western blot analysis (right panel) of purified vector. PM stands for protein marker, M is monomer, and D is dimer. (b) Hemolytic activity of the dimer with various concentrations at pH 7.4, 7.0, and 5.0.

(Figure 5a). At 2.8 nM ligand concentration, almost complete inhibition of the transfection was achieved.

In addition, to demonstrate targeted delivery of the nanoparticles, the vector/pEGFP complexes at the optimum N:P ratio of 10 were used to transfect ZR-75-1 and MDA-MB-231 breast cancer cells and MCF-10A normal mammary cells. The results showed that 16 ± 1% of the ZR-75-1 cells were transfected in comparison to 0.01 ± 0.004 and 0.6 ± 0.1% for MCF-10A and MDA-MB-231 cells, respectively (Figure 5b). Lipofectamine transfected nonselectively all cell lines with relatively high efficiency.

3.7. Evaluation of the Functionality of EDM and NLS. To study the ability of the vector to efficiently disrupt endosome membranes, ZR-75-1 cells were transfected in the presence of bafilomycin A1 and chloroquine. The results of the transfection studies in the presence and absence of bafilomycin A1 showed significant reduction in total green fluorescent protein expression from 45,000 ± 7,800 to 4,100 ± 2,700 AFU (arbitrary fluorescence units) (Figure 6a). The percent transfected cells was also significantly reduced from 16 ± 1 to 4 ± 0.7 in the absence and presence of bafilomycin A1, respectively. In the presence of chloroquine, no significant increase in transfection efficiency was observed (Figure 6a).

The role of microtubules in facilitating translocation of nanoparticles toward nucleus was evaluated by transfecting cells in the presence of nocodazole. The results revealed significant reduction in gene expression from 45,000 ± 7,800 to 5,200 ± 2,300 AFU when microtubule networks were disrupted by nocodazole. The percent transfected cells was also significantly reduced from 16 ± 1 to 3 ± 0.4 in the absence and presence of nocodazole, respectively (Figure 6b).

The impact of NLS in the vector structure on transfection efficiency was further studied by transfecting ZR-75-1 cells with DBV (dimer) and DBV without NLS. The results demonstrated significant reduction in transfection efficiency from 45,000 ± 7,800 to 11,500 ± 2,300 AFU when vector without NLS was used (Figure 6b).

3.8. Cancer Cell Killing Efficiency. The vector related toxicity was measured by transfecting ZR-75-1 cells with vector only or vector in complex with pEGFP. The results exhibited no significant cell toxicity related to the vector or vector in complex with pEGFP at an N:P ratio of 10 (Figure 7). The potential of the vector in delivering plasmid DNA encoding TRAIL (tumor-related apoptosis inducing ligand) for cancer gene therapy was demonstrated by transfecting ZR-75-1 cells with the vector/pTRAIL-GFP complexes. Up to 62% of the cells died when treated with one dose of vector/pTRAIL-GFP complexes. Lipofectamine in complex with pTRAIL-GFP was used as a control and resulted in killing up to 50% of the cancer cells, which was significantly lower than for vector/pTRAIL-GFP complexes (Figure 7).

4. Discussion

During the evolution process, nature has designed various motifs that can efficiently condense DNA (e.g., histones and virus DNA condensing peptides),[11,15] disrupt endosomes (e.g., adenovirus fusogenic peptide and mellitin),[16,17] or actively translocate genetic materials to the cell nucleus (e.g.,

(15) Haberland, A.; Cartier, R.; Heuer, D.; Zaitsev, S.; Paulke, B. R.; Schafer-Korting, M.; Bottger, M. Structural aspects of histone H1-DNA complexes and their relation to transfection efficiency. *Biotechnol. Appl. Biochem.* **2005**, *42*, 107–17.

(16) Boeckle, S.; Fahrmeir, J.; Roedl, W.; Ogris, M.; Wagner, E. Melittin analogs with high lytic activity at endosomal pH enhance transfection with purified targeted PEI polyplexes. *J. Controlled Release* **2006**, *112*, 240–8.

(17) Subramanian, A.; Ma, H.; Dahl, K. N.; Zhu, J.; Diamond, S. L. Adenovirus or HA-2 fusogenic peptide-assisted lipofection increases cytoplasmic levels of plasmid in nondividing endothelium with little enhancement of transgene expression. *J. Gene Med.* **2002**, *4*, 75–83.

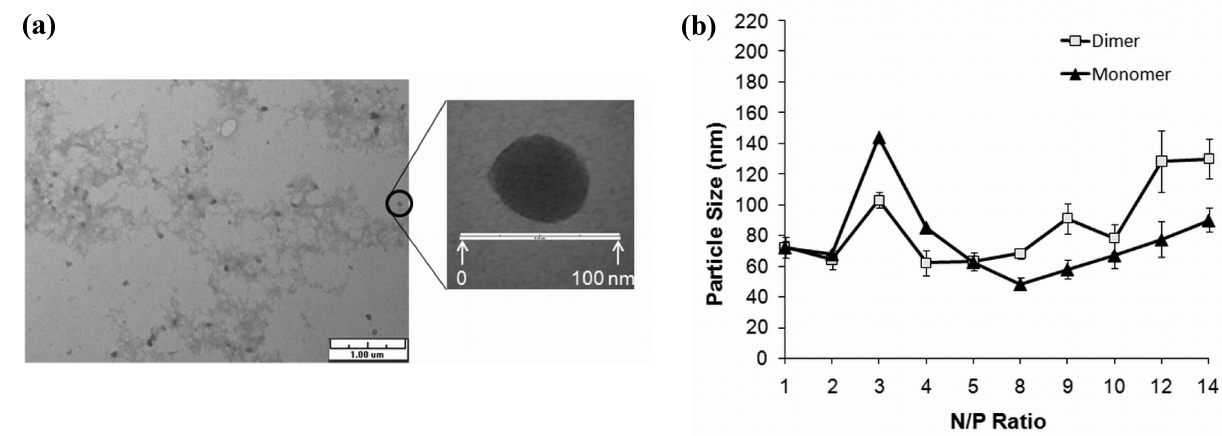

Figure 3. Nanoparticle shape and size analysis. (a) The TEM picture of the spherical nanoparticles formed at N:P 10. (b) The particle size analysis of vector/pEGFP complexes formed with monomer and dimer at various N:P ratios.

adenovirus nuclear localization signal).[18] The objective of this research was to examine the possibility of packaging multiple natural motifs with diverse functions into one vector while preserving the functionality of each.

Using genetic engineering techniques, a multidomain biomimetic vector was designed, cloned, and expressed in both monomer and dimer configurations (Figure 2a).

We characterized the vector in terms of its pH and concentration dependent membrane disrupting activity by incubating the vector with red blood cells. It was observed that the membrane disrupting activity of the vector significantly increased as pH decreased (Figure 2b). The endosome disrupting motif used in this study was first developed by Monsigny's group,[13] namely, 5HWYG. It mimics the endosome disrupting activity of fusogenic peptide in influenza virus but at a pH close to 6.9. The pH change causes the EDM to change conformation into α-helical structure, fuse with the early endosome membranes, and escape into the cytoplasm. At pH 7.0, the fusogenic peptide seems to have partially changed conformation into α-helical structure. As a result, at low concentrations the hemolytic activity is insignificant whereas it becomes prominent at higher concentrations. Therefore it can be construed that as the number of vector molecules used to complex with one pDNA molecule increases, the endosome disrupting efficiency of the nanoparticles could increase. These features of EDM, the pH and concentration dependence membrane disrupting activities are extremely important as they minimize the possibility of causing unintended cell damage while in contact with normal cell membranes. So far, we have characterized the vector in terms of expression, purity and membrane disrupting activity. The next logical step is to examine the ability of the vector to complex with pDNA followed by physicochemical and biological characterization.

In the vector structure we have utilized arginine rich adenovirus μ peptide[19] to complex with pDNA and form condensed nanosize particles. To examine the extent of pDNA condensation, vectors were complexed with pEGFP and characterized in terms of size by dynamic light scattering technique and shape by transmission electron microscopy. The TEM images and particle size analysis results showed that the vectors were able to efficiently condense pEGFP into nanoparticles in the size range that is suitable for receptor mediated endocytosis (i.e., <150 nm) (Figures 3a and 3b).[20]

Nanoparticles were further characterized in terms of their ability to mediate gene transfer into the ZR-75-1 model breast cancer cell line in order to identify the optimum N:P ratio for transfection. This cell line was selected because the model targeting peptide used in the vector structure was developed through combinatorial screening to specifically target this cell line with minimal binding affinity toward normal mammary cells.[12] The identity of the receptor to which the targeting peptide binds is unknown at this point but under investigation by others.[12] As a positive control we used Lipofectamine to validate the transfection protocol. It is noteworthy that commercially available transfection reagents such as Lipofectamine (nontargeted) are usually formulated to flocculate into large size particles so that they can precipitate readily onto the cell surface for maximum transfection efficiency. Such nontargeted systems may not be suitable for systemic gene delivery due not only to their nonspecific binding to normal cells but also to their large size. For targeted nanoparticles, size plays an extremely important role in mediating efficient gene transfer because it has been shown that only particles with sizes less than 200 nm can fit into clathrin-coated vesicles.[20] Since we did not observe any significant difference between the tranfsection efficiency of dimer versus monomer (Figure 4a), we proceeded with the characterization of dimer which holds a more complex architecture.

(18) Escriou, V.; Carriere, M.; Scherman, D.; Wils, P. NLS bioconjugates for targeting therapeutic genes to the nucleus. *Adv. Drug Delivery Rev.* **2003**, *55*, 295–306.

(19) Tecle, M.; Preuss, M.; Miller, A. D. Kinetic study of DNA condensation by cationic peptides used in nonviral gene therapy: analogy of DNA condensation to protein folding. *Biochemistry* **2003**, *42*, 10343–7.

(20) Rejman, J.; Oberle, V.; Zuhorn, I. S.; Hoekstra, D. Size-dependent internalization of particles via the pathways of clathrin- and caveolae-mediated endocytosis. *Biochem. J.* **2004**, *377*, 159–69.

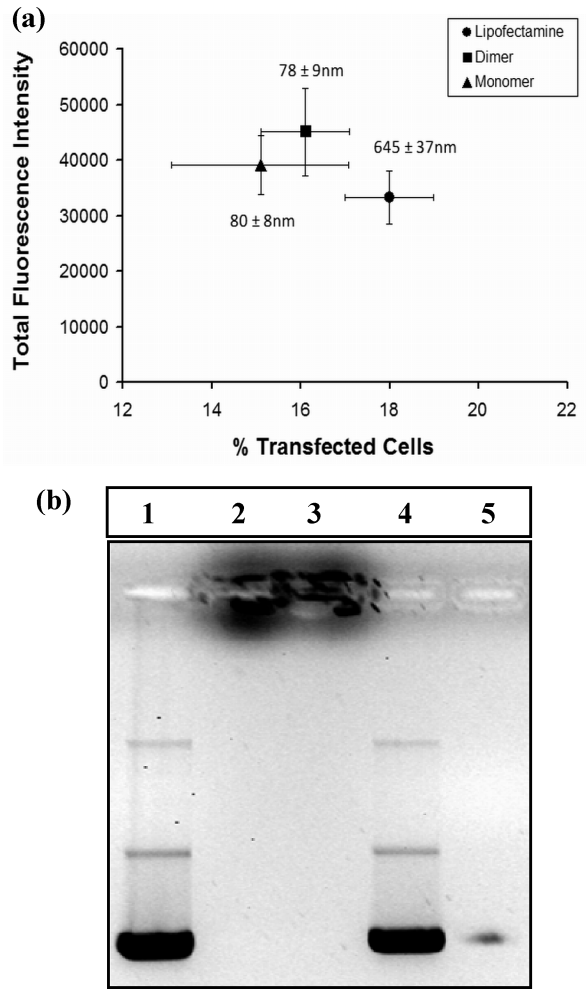

Figure 4. Nanoparticle characterization in terms of mediating gene transfer and stability. (a) Gene transfection efficiency of monomer (N:P 10), dimer (N:P 10), and Lipofectamine. pEGFP was used as a model reporter gene. The corresponding nanoparticle size is also reported. (b) Gel retardation assay of pDNA and vector/pDNA complexes at N:P 10. Lane 1: pDNA in the absence of serum. Lane 2: Vector/pDNA complexes in the absence of serum. Lane 3: Vector/pDNA complexes incubated with serum. Lane 4: Released pDNA from the vector/pDNA complexes after incubation with serum. Lane 5: pDNA incubated with 10% serum for 30 min.

To examine whether the vector is able to protect pDNA from serum endonucleases, nanoparticles were incubated with serum. The observations indicate that the vector not only has the potential to efficiently protect the pDNA from plasma endonucleases but also could maintain its integrity until reaching the target cells (Figure 4b).

We also performed an inhibition assay to evaluate the functionality of the targeting motif in the vector structure and the internalization of nanoparticles via receptor-mediated endocytosis. This was done by pretreatment of ZR-75-1 cells with the targeting peptide to saturate the receptors followed by transfection of the cells with vector/pEGFP complexes. The inverse relationship between ligand concentration and total GFP expression indicates that addition of the targeting peptide to the media blocks internalization of the targeted nanoparticles resulting in lower levels of gene expression (Figure 5a). This also means that the nanoparticles were internalized via the receptors that were blocked by the targeting peptide.

To demonstrate targeted delivery of the nanoparticles, the vector/pEGFP complexes at the optimum N:P ratio of 10 were used to transfect ZR-75-1 and MDA-MB-231 breast cancer and MCF-10A normal mammary cells. The results showed that the percent transfected cells for MCF-10A and MDA-MB-231 cells were significantly lower than for ZR-75-1 (Figure 5b). This can be attributed to the absence of the necessary receptors on the surface of MCF-10A and MDA-MB-231 cells for the targeting peptide. It also suggests that the targeting peptide facilitated receptor-mediated internalization of the nanoparticles in ZR-75-1 cells with no significant internalization in normal mammary cells. This finding was expected as the targeting peptide in the vector structure was developed by a bacterial display system (combinatorial screening) to specifically target ZR-75-1 but not MCF-10A cells.[12]

We then asked the question whether the EDM in the vector structure played a role and had a significant effect on the endosomal escape and subsequent transgene expression. The designed fusogenic peptide is expected to effectively increase the delivery of pDNA into the cytosol via membrane destabilization of acidic endocytotic vesicles containing vector/pDNA complexes. This was assessed by transfecting ZR-75-1 cells in the absence and presence of bafilomycin A1 and chloroquine. Choloroquine is a buffering agent known to disrupt the endosomal membrane by increasing the pH of the endosome environment.[21] In contrast, bafilomycin A1 is an inhibitor of vacuolar ATPase endosomal proton pump which prevents the escape of the cargo into cytosol by inhibiting the acidification of the endosome environment.[22] The significant reduction in transfection efficiency in the presence of bafilomycin A1 highlights the fact that the acidification of the endosomal compartment is necessary for the escape of the nanoparticles into cytosol (Figure 6a). These results in combination with the results obtained from the hemolysis assay suggest that EDM played a significant role in enhancing gene expression due to its pH-dependent fusogenic activity. Interestingly, in the presence of chloroquine, no significant increase in transfection efficiency was observed (Figure 6a). This observation supports the hypothesis that the EDM motif preserves its functional integrity and assists the nanoparticles in efficient escape from the endosomes. It is plausible that this significant endosome disrupting activity is the result of additive or synergistic effects of fusogenic peptide and histidine residues in the vector structure. Because we have designed a histag

(21) Salem, A. K.; Searson, P. C.; Leong, K. W. Multifunctional nanorods for gene delivery. *Nat. Mater.* **2003**, *2*, 668–71.
(22) Bowman, E. J.; Siebers, A.; Altendorf, K. Bafilomycins: a class of inhibitors of membrane ATPases from microorganisms, animal cells, and plant cells. *Proc. Natl. Acad. Sci. U.S.A.* **1988**, *85*, 7972–6.

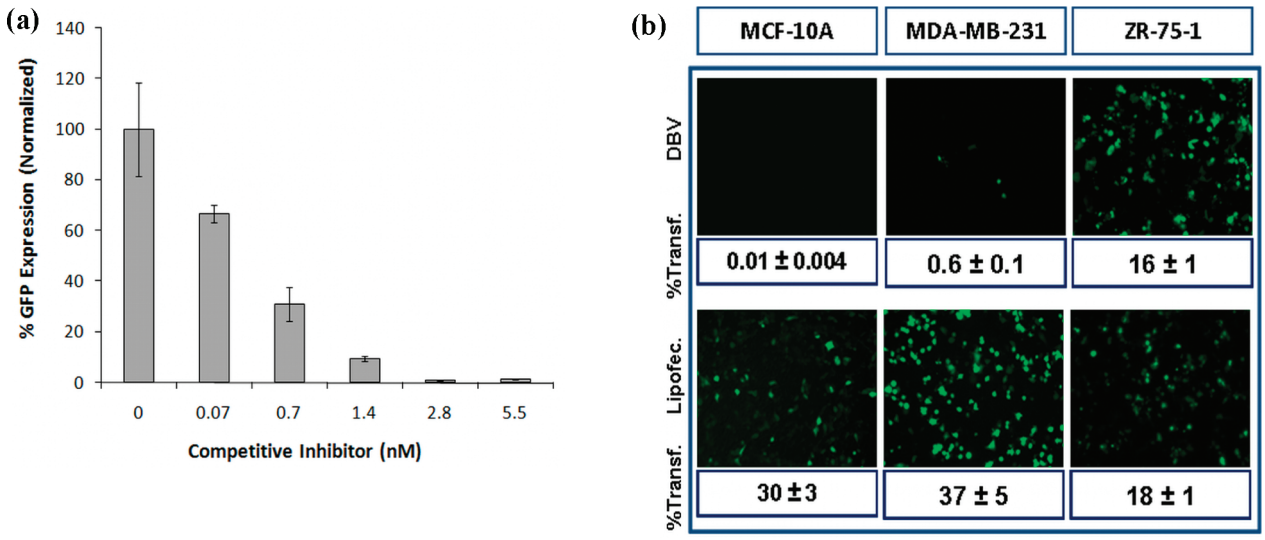

Figure 5. Evaluation of the functionality of targeting peptide in dimer. (a) Internalization of nanoparticles via receptor-mediated endocytosis is demonstrated by an inhibition assay. Targeting peptide at various concentrations was used as a competitive inhibitor. (b) Epifluorescent images and percentage of the MCF-10A, MDA-MB-231 and ZR-75-1 cells transfected with vector/pEGFP complexes at an N:P ratio of 10 and Lipofectamine. The percentage of transfected cells was measured by flow cytometry.

in the vector sequence to facilitate purification of the vector from the *E. coli*, it could have contributed to the disruption of endosomes via the proton sponge effect.[23,24] It is also noteworthy that EDM and DCM contain 5 and 3 histidine residues in their sequences, respectively. Therefore, the presence of 14 histidines out of 95 amino acid residues in the vector sequence along with the fusogenic peptide could be the reason for the efficient endosome membrane disruption. More in depth studies on this finding are needed to better understand this phenomenon.

Although there is limited understanding of the cellular and molecular mechanisms involved with synthetic vector mediated gene transfer, transfection efficiency seems to be fundamentally limited by inefficient trafficking of DNA from the cytosol to the site of gene transcription in the nucleus.[25] To overcome this obstacle, we utilized the NLS from the *Rev* protein (residues 35−51) of human immunodeficiency virus (HIV) and engineered the signal sequence at the vector's N-terminal to promote the transport of nanoparticles via microtubules across the cytoplasm toward the nucleus. Presence of the NLS in the vector structure could reduce the cytosolic residence time and increase the probability of accumulation of nanoparticles inside the nucleus through either the nuclear pore complex or during the mitosis phase of cell cycle. For nanoparticles with diameter smaller than 30 nm the possibility of entering the nucleus via the nuclear pore complex exists, however bigger particles are more likely to enter the nucleus during the mitosis phase when nuclear membrane dissolves. To investigate the effect of microtubules on the translocation of pDNA to the nucleus, ZR-75-1 cells were transfected in the presence and absence of nocodazole, a reagent known to depolymerize microtubule structures.[26] The results revealed significant reduction in gene expression when the microtubule network was disrupted (Figure 6b). Therefore, it can be deduced that the nanoparticles exploited microtubules to reach the nucleus. Furthermore, we examined whether the presence of NLS in the vector structure had any significant impact on enhancing gene transfer efficiency. This was achieved by transfecting ZR-75-1 cells with the DBV that did not have NLS in its structure. In comparison to DBV, there was an approximately 75% reduction in the expression of GFP in the DBV lacking NLS (Figure 6b). This indicates that the presence of the NLS had a significant role in the nanoparticles reaching the nucleus.

So far, we have examined each motif in the vector structure and have shown that, by correct positioning in the vector backbone, the functionality of each motif can be preserved. This can be explained by the fact that, during the pDNA condensation process, hundreds of vector molecules participate to condense one molecule of pDNA. For example, at an N:P ratio of 10, more than 2200 vector molecules are employed to condense one pEGFP molecule (9462 negative charges). Therefore, it is probable to have a fraction of fully functional targeting motifs, NLSs, and EDMs in the vector/pDNA complex architecture. Thus, the nanocomplex is rendered ready to bind to the receptors, fuse with the

(23) Behr, J. P. The proton sponge: A trick to enter cells the viruses did not exploit. *Chimia* **1997**, *51*, 34–36.

(24) Shigeta, K.; Kawakami, S.; Higuchi, Y.; Okuda, T.; Yagi, H.; Yamashita, F.; Hashida, M. Novel histidine-conjugated galactosylated cationic liposomes for efficient hepatocyte-selective gene transfer in human hepatoma HepG2 cells. *J. Controlled Release* **2007**, *118*, 262–70.

(25) Suh, J.; Wirtz, D.; Hanes, J. Efficient active transport of gene nanocarriers to the cell nucleus. *Proc. Natl. Acad. Sci. U.S.A.* **2003**, *100*, 3878–82.

(26) Suh, J.; Wirtz, D.; Hanes, J. Real-time intracellular transport of gene nanocarriers studied by multiple particle tracking. *Biotechnol. Prog.* **2004**, *20*, 598–602.

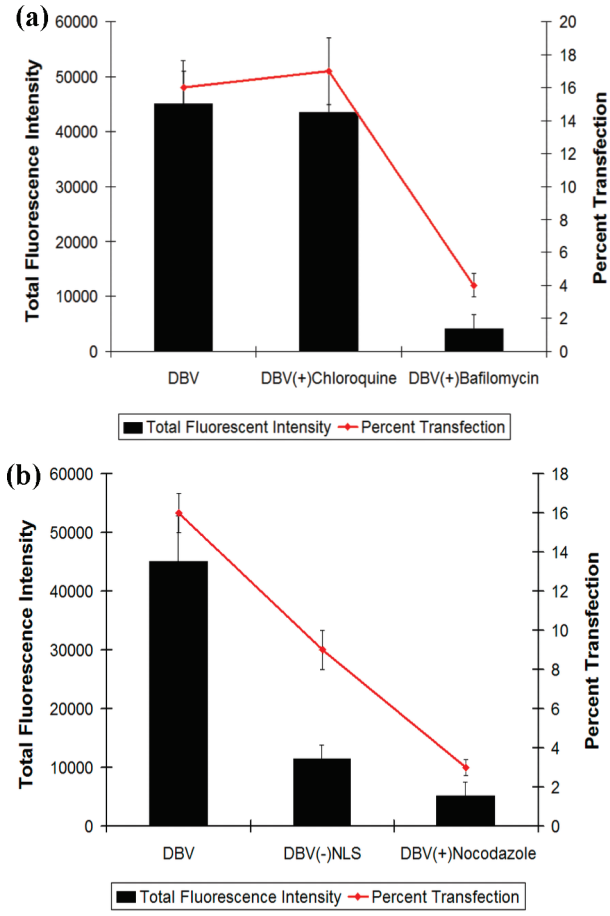

Figure 6. Evaluation of the functionality of EDM and NLS. (a) Quantitative measurements of the total gene expression as well as percent trasfected cells for the ZR-75-1 in the presence and absence of chloroquine (CQ) and bafilomycin A1. (b) Measurement of total green fluorescent protein expression for ZR-75-1 cells transfected with the DBV, DBV without NLS and DBV in the presence of nocodazole.

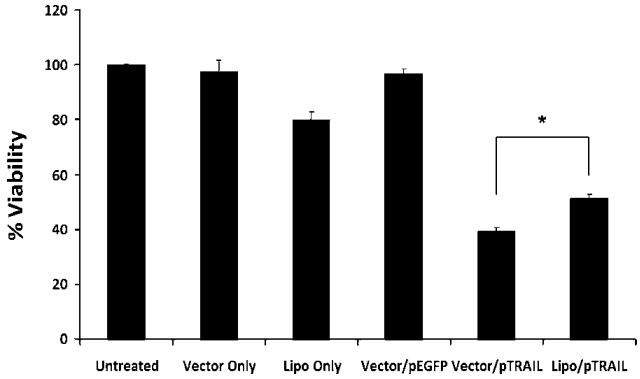

Figure 7. Evaluation of the cancer cell killing efficiency of the vector/pTRAIL-GFP complexes using WST-1 cell toxicity assay. Vector alone, Lipofectamine alone, vector/pEGFP complexes and Lipofectamine/pTRAIL-GFP complexes were used as controls.

endosome membranes, and utilize the microtubules for active translocation of genetic material to the cell nucleus.

One important question that we asked was whether this level of transfection efficiency is sufficient to mediate significant therapeutic outcome. We have deliberately chosen a highly specific targeting peptide which is customized for ZR-75-1 cells. In Figure 4a we showed that approximately 16% of the cells can be transfected with high levels of gene expression. Based on this observation, we selected a therapeutic molecule named TRAIL (tumor necrosis factor related apoptosis inducing ligand) as a model drug. TRAIL was selected because of its bystander effect as well as relative sensitivity of ZR-75-1 cells to this molecule.[27,28] To examine the therapeutic potential of the vector in delivering TRAIL, ZR-75-1 cells were incubated with the vector alone, vector in complex with pEGFP and vector in complex with pTRAIL-GFP. The results exhibited no significant cell toxicity related to the vector or vector in complex with pEGFP (Figure 7). However, up to 62% of the cells died when treated with vector/pTRAIL-GFP. This means that for every single cell that was killed after transfection with pTRAIL, three additional neighboring cells died as a result of the bystander effect. Application of other therapeutic molecules which possess higher levels of bystander effect could result in more significant cell death. Thus, achievement of significant therapeutic outcomes is based not only on percent transfected cells, but on the level of gene expression and proper selection of therapeutic molecules.

One last question that we asked was why all the cells were not transfected, even though the vector seems to have overcome the major known cellular barriers. Besides the administered pDNA dose, the answer could be as simple as the fact that the abundance of entry gates (i.e., receptors) on the surface of cancer cells dictates the number of particles that can be internalized. Viruses such as adenovirus are a good example as they are able to transfect various cell lines with different transfection efficiencies depending on the number of coxsackie adenovirus receptor present on the surface of the cells.[29] In addition, not all ZR-75-1 cancer cells overexpress the receptors required for the internalization of the nanoparticles because cancer cell populations are usually heterogeneous. Nonetheless, other more complex reasons may be involved which calls for more mechanistic studies to unravel the mysteries of efficient gene transfer.

(27) Kagawa, S.; He, C.; Gu, J.; Koch, P.; Rha, S. J.; Roth, J. A.; Curley, S. A.; Stephens, L. C.; Fang, B. Antitumor activity and bystander effects of the tumor necrosis factor-related apoptosis-inducing ligand (TRAIL) gene. *Cancer Res.* **2001**, *61*, 3330–8.

(28) Singh, T. R.; Shankar, S.; Chen, X.; Asim, M.; Srivastava, R. K. Synergistic interactions of chemotherapeutic drugs and tumor necrosis factor-related apoptosis-inducing ligand/Apo-2 ligand on apoptosis and on regression of breast carcinoma in vivo. *Cancer Res.* **2003**, *63*, 5390–400.

(29) Li, D.; Duan, L.; Freimuth, P.; O'Malley, B. W., Jr. Variability of adenovirus receptor density influences gene transfer efficiency and therapeutic response in head and neck cancer. *Clin. Cancer Res.* **1999**, *5*, 4175–81.

5. Conclusion

We have demonstrated that a multidomain designer vector with a complex chimeric architecture can retain individual functionality of its constituents. There is an increasing body of evidence that proteins are more flexible than previously thought and can retain functional integrity in multiple conformations, thus, boosting the possibility of successful *in vitro* evolution of complex designer macromolecules.[30] This would allow creation of efficient and targeted systems that can be fine-tuned for various gene delivery needs. Such systems can be equipped with a variety of cell specific targeting motifs and used to transfer genes to various cell types with potential applications in gene therapy for cancer, cardiovascular disease, wound healing, and many others.

Acknowledgment. This work was funded by the Department of Defense Breast Cancer Concept Award W81XWH-07-1-0533 (BC062929).

MP800251X

(30) Murzin, A. G. Biochemistry. Metamorphic proteins. *Science* **2008**, *320*, 1725–6.